

## Plasmas on Quantized Accumulation Layers on ZnO Surfaces

A. Many, I. Wagner, and A. Rosenthal

*The Racah Institute of Physics, The Hebrew University of Jerusalem, Jerusalem 91000, Israel*

and

J. I. Gersten

*Institute for Advanced Study, The Hebrew University of Jerusalem, Jerusalem 91000, Israel, and*

*Department of Physics, City College of the City University of New York,<sup>(a)</sup>*

*New York, New York 10031*

and

Y. Goldstein<sup>(b)</sup>

*Exxon Research and Engineering Company, Linden, New Jersey 07036*

(Received 6 February 1981)

Low-energy—electron-loss spectroscopy is used to study collective surface excitations on accumulation layers on ZnO. A prominent loss peak is observed which shifts in energy with electron concentration. The results are well accounted for theoretically and provide direct evidence for the existence of two-dimensional plasmons.

PACS numbers: 71.45.Gm, 73.20.-r, 79.20.Kz

The elementary collective excitations of solid surfaces play a fundamental role in a number of recently discovered phenomena. These include some novel device applications like the generation of far-infrared radiation,<sup>1</sup> surface photochemistry,<sup>2</sup> and surface-enhanced adsorbate spectroscopy.<sup>3</sup> The primary tools for probing such excitations have been optical. While optical spectroscopy yields excellent energy resolution, its spatial resolution is limited by its wavelength. In this Letter we report a study of surface excitations by low-energy—electron-loss spectroscopy (LEELS). We present experimental data for LEELS on ZnO surfaces and interpret the data theoretically. The surface properties of ZnO are changed by varying the electron density in the accumulation layer. The elementary excitations consist of coupled two-dimensional (2D) plasmon and phonon modes.

The possibility of 2D plasmas in quantized space-charge layers was first pointed out by Stern<sup>4</sup> in 1967, but their detection was found to be experimentally quite difficult. To attain the quantized space-charge layers one usually works with the silicon metal-oxide-semiconductor (MOS) structure, where the silicon is not very amenable to direct exterior probes. Thus experimental evidence for the existence of 2D plasmons on MOS structures was found only recently.<sup>5,6</sup>

LEELS was developed<sup>7</sup> to probe the electronic excitations at the surface and is natural for the study of 2D plasmas, provided that one can produce a quantized space-charge layer on a *free* surface. We performed our measurements on

ZnO surfaces, one of the few semiconductors where quantized accumulation layers on the free surface can be obtained with relative ease.<sup>8-10</sup> Our preliminary results<sup>11</sup> contained a coarse background in the energy-loss spectra which was attributed to scattering by 2D plasmons. The present improved data show a pronounced peak due to the plasmons. The energy of the peak increases monotonically with the surface electron concentration  $N_s$ . Measurements were performed up to  $N_s \approx 2 \times 10^{13} \text{ cm}^{-2}$ , about an order of magnitude higher than on silicon.

The theory of 2D plasmas in ZnO—a polar crystal—is somewhat more complicated than in silicon. The plasmon mode couples to the surface and bulk phonon modes and forms three hybrid branches, termed plasmarons.<sup>12</sup> Some theoretical studies of electron scattering from solid surfaces have appeared in the literature.<sup>7</sup> In our previous work<sup>11</sup> we developed a theory for ZnO in which the coupling to the plasmaron modes of the surface was manifest. A number of approximations were made, however, making a detailed comparison between theory and experiment difficult. These limitations have now been removed. Thus, in this Letter, all three branches of the plasmaron spectrum<sup>12</sup> are included, rather than just the bare two-dimensional plasmon. We also generalize the formalism to include azimuthal, elastic, and sequential multiple scattering; plasmaron absorption and emission processes; and instrumental resolution effects.

The measurements were made on the “oxygen” (0001) face of ZnO single crystals, grown by the

Airtron Company with use of the hydrothermal method. The surface was cleaned by repeated argon bombardments at a pressure of 1 mTorr and a temperature of 200 °C, and annealed at 500 °C. Accumulation layers were produced by exposure to atomic hydrogen<sup>8</sup> and removed by exposure to oxygen.

Because the surface mobility  $\mu$  could not be measured in the present configuration, we used

$$\left(\frac{dP}{d\Omega' d\epsilon'}\right)_{\text{in}} = \frac{m^2 |R_0|^2}{\hbar^4 \pi^2} \sum_{\lambda} |\gamma_{\kappa\lambda}|^2 (\epsilon'/\epsilon)^{1/2} \left| \frac{\kappa}{\kappa^2 + (P_z' - P_z)^2} \right|^2 \times [(N_{\kappa\lambda} + 1) \delta(\epsilon - \epsilon' - \hbar\omega_{\kappa\lambda}) + N_{\kappa\lambda} \delta(\epsilon - \epsilon' + \hbar\omega_{\kappa\lambda})], \quad (1)$$

where  $\gamma_{\kappa\lambda}$  is the coupling constant<sup>12</sup> to a plasmaron of 2D wave vector  $\vec{\kappa}$ , branch  $\lambda$  ( $\lambda = -1, 0, +1$ ), and energy  $\hbar\omega_{\kappa\lambda}$ .  $N_{\kappa\lambda}$  is the Bose factor and  $R_0$  is the elastic reflection amplitude. Equation (1) is similar to Eq. (19) of Ref. 11, but here the anti-Stokes plasmaron absorption process (the second term in the square brackets) is now also included. The incident and scattered electron energies are denoted by  $\epsilon$  and  $\epsilon'$ , respectively. The elastic scattering probability is  $|R_0|^2 \delta(\epsilon - \epsilon') \delta(\theta - \theta') \delta(\varphi - \varphi') / \sin\theta'$ , where  $\theta$  and  $\theta'$  are the angles of the primary and the scattered beam with the surface normal, respectively, while  $\varphi$  and  $\varphi'$  are the azimuthal angles. Since the net parallel momentum for the near specular beam is conserved, we have

$$\kappa^2 = (2m/\hbar^2) [\epsilon \sin^2\theta + \epsilon' \sin^2\theta' - 2(\epsilon\epsilon')^{1/2} \sin\theta \sin\theta' \cos(\varphi - \varphi')] \approx (2m\epsilon/\hbar^2) \{[\delta\theta \cos\theta \mp (\hbar\omega_{\kappa\lambda}/2\epsilon) \sin\theta]^2 + (\delta\varphi \sin\theta)^2\}, \quad (2)$$

where  $\delta\theta = \theta' - \theta$ ,  $\delta\varphi = \varphi' - \varphi$ , and the negative sign (positive sign) applies to the emission (absorption) process. Introducing a Gaussian energy-resolution function for the monochromator and analyzer, the

the values of  $\mu N_s$  to characterize the accumulation layers. These values were derived from the measured surface conductance, once we assumed that the "zinc" and "oxygen" faces contribute equally to the conductance. We estimate that our highest experimental  $N_s$  values were around  $(2-3) \times 10^{13} \text{ cm}^{-2}$ .

An expression for the probability that an electron will be inelastically scattered into a given solid angle and energy range is

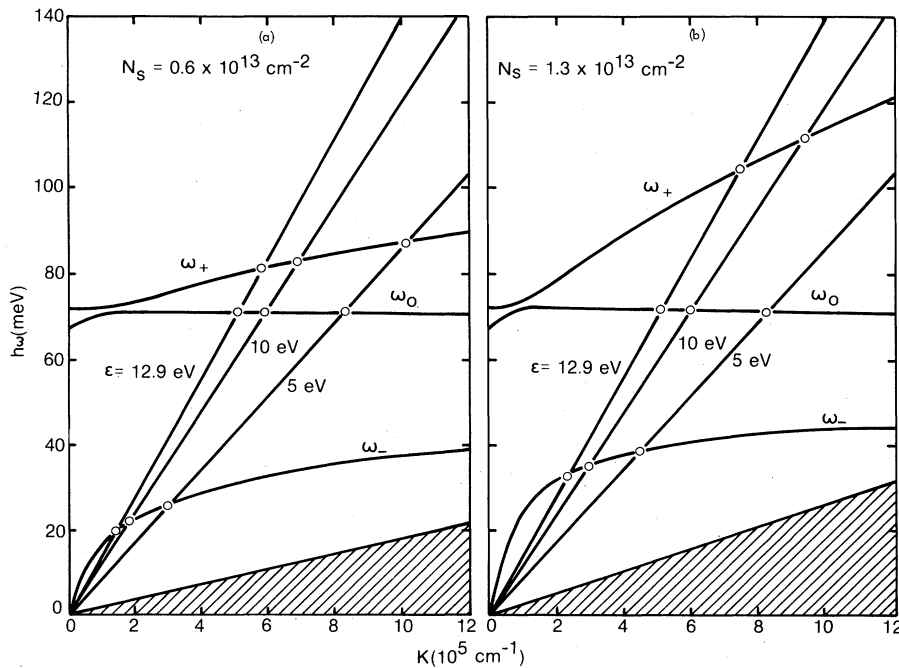


FIG. 1. Calculated collective excitation spectra for a 2D electron gas on the surface of ZnO.

total scattering probability per unit energy becomes

$$\frac{dP}{d\epsilon'} = \frac{|R_0|^2}{\Delta(2\pi)^{1/2}} \left[ \exp[-(\epsilon' - \epsilon)^2/2\Delta^2] + (4\pi\epsilon^2)^{-1} \int d\Omega' \sum_{\lambda} \frac{|K\gamma_{\kappa\lambda}|^2}{[(\delta\theta)^2 + (\hbar\omega_{\kappa\lambda}/2\epsilon)^2 + (\sin\theta\delta\varphi)^2]^2} \right. \\ \left. \times \{(N_{\kappa\lambda} + 1) \exp[-(\epsilon - \epsilon' - \hbar\omega_{\kappa\lambda})^2/2\Delta^2] + N_{\kappa\lambda} \exp[-(\epsilon - \epsilon' + \hbar\omega_{\kappa\lambda})^2/2\Delta^2]\} \right], \quad (3)$$

where  $2.4\Delta$  is the full energy-resolution width at half maximum. Sequential multiple plasmaron emission and/or absorption results in terms involving multiple autoconvolutions of the spectrum of Eq. (3).

In Fig. 1 we plot calculated collective excitation spectra for a 2D electron gas on the ZnO surface for two values of  $N_s$ . The curves labeled  $\omega_+$ ,  $\omega_0$ , and  $\omega_-$  represent the three plasmaron branches. Notice that for the higher value of  $N_s$  the upper and the lower branches ( $\omega_+$  and  $\omega_-$ ) increase more rapidly as a function of the 2D wave vector. The electron-hole pair excitation region is also shown by the shaded area at the bottom of the figures.

The straight lines in the figures, commencing at the origin, represent Eq. (2) for the case of complete specularity ( $\delta\theta = \delta\varphi = 0$ ) and correspond to different incident electron energies, as marked. The intersections of these lines with the plasmaron dispersion curves ( $\omega_+$ ,  $\omega_0$ , and  $\omega_-$ ) determine the  $(\omega, \kappa)$  values involved in the inelastic scattering process at specular reflection. For nonperfect specular scattering (finite admission angle) the points of intersection spread into sizable segments of the dispersion curves.

In Fig. 2 we present the measured LEELS data (full lines) at the ZnO surface for an incident electron energy of 12.9 eV and for three values of  $\mu N_s$ :  $N_s = 0$  (no accumulation layer), and for  $\mu N_s = 1.1 \times 10^{15}$  and  $4.0 \times 10^{15}$  (V sec) $^{-1}$ , both corresponding to quantized accumulation layers. The most distinctive feature of the experimental curves, apart from the main peak at zero energy loss (elastic scattering), is a pronounced loss peak. At  $N_s = 0$  this loss peak appears at  $\sim 65$  meV and corresponds to the unperturbed surface phonon,<sup>7,11</sup> but as  $N_s$  increases, the peak shifts to higher energies. Now this peak is due to scattering by 2D plasmons and corresponds to energy losses to the upper plasmaron branch ( $\omega_+$ ).

The two dashed curves in the figure show the theoretical scattering probability calculated from Eq. (3) for  $N_s$  values of  $6 \times 10^{12}$  and  $1.3 \times 10^{13}$  cm $^{-2}$ . Again we see a prominent  $\omega_+$  peak. Losses to the  $\omega_-$  and  $\omega_0$  branches are not resolved as separate peaks due to instrumental resolution, weaker coupling,<sup>12</sup> and lifetime broadening. In addition, the dashed curves also take into account the subse-

quent emission (absorption) of up to two plasmarons. As can be seen, the theoretical curves are in good agreement with the experimental ones. They reproduce correctly the positions of the loss peaks even though they predict a somewhat higher amplitude. (In regions where the dashed curves coincide with the measured ones, only the full lines are shown.)

The energy dependence of the experimental loss peak (circles and triangles) on  $\mu N_s$  is shown in the inset of Fig. 2. For comparison with theory we have used two mobility values; a "bulk" value of 200 cm $^2$ /V sec and the value of 100 cm $^2$ /V sec measured<sup>13</sup> on "real" surfaces. We see that the

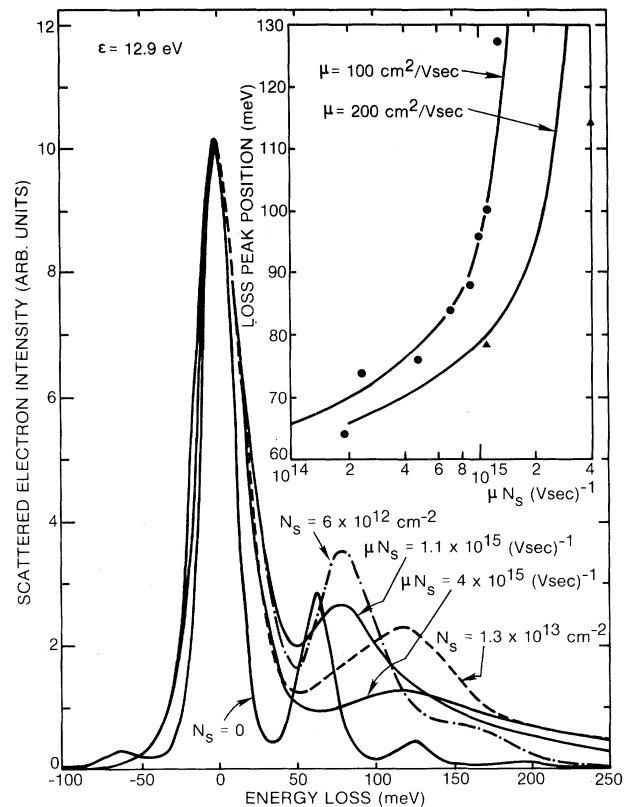


FIG. 2. Experimental LEELS spectra (solid lines) with corresponding theoretical curves (dashed lines). The inset compares the experimental loss peaks for two crystals (circles and triangles) with theory (solid lines).

circles are in good agreement with the latter curve, while the triangles are closer to the other curve. The triangles represent measurements on a different crystal where the mobility may have been higher. Within the uncertainty in the mobility, the experimental data and the theoretical curves are seen to be in fair agreement.

The data in Fig. 2 provide, to our knowledge, the most direct experimental evidence for the existence of 2D plasmons on solid surfaces. The overall agreement between theory and experiment, and especially the reproduction by the theory of the plasmon peak at the right location, substantiates the theory and leaves little doubt that the peak is due mainly to the uppermost plasmaron branch ( $\omega_+$ ). (In quantized accumulation layers this branch is predominately plasmonlike, analogous to the "bare" plasmon observed<sup>5,6</sup> in nonpolar semiconductors.) However, all three plasmaron branches are needed to account for the features of the experimental spectrum.

In conclusion, we demonstrated the existence of 2D plasma oscillations in quantized accumulation layers on ZnO surfaces. The good agreement between the plasmaron dispersion relations and the experimental results supports the concepts underlying the theory.

The authors wish to acknowledge the important contribution of Dr. R. E. Kirby in the construction of the electron spectrometer.

<sup>(a)</sup>Present address.

<sup>(b)</sup>Permanent address: Racah Institute of Physics, The Hebrew University of Jerusalem, Jerusalem 91000, Israel.

<sup>1</sup>D. C. Tsui, E. Gornick, and R. A. Logan, *Solid State Commun.* **35**, 875 (1980).

<sup>2</sup>A. Nitzan and L. E. Brus, to be published.

<sup>3</sup>J. I. Gersten and A. Nitzan, *J. Chem. Phys.* **73**, 3023 (1980).

<sup>4</sup>F. Stern, *Phys. Rev. Lett.* **18**, 548 (1967).

<sup>5</sup>S. J. Allen, Jr., D. C. Tsui, and R. A. Logan, *Phys. Rev. Lett.* **38**, 980 (1977).

<sup>6</sup>See also a review article by T. N. Theis, *Surf. Sci.* **98**, 515 (1980).

<sup>7</sup>See the review article by H. Froitzheim, in *Electron Spectroscopy for Surface Analysis*, Topics in Current Physics, Vol. 4, edited by H. Ibach (Springer, Berlin, 1977), p. 205.

<sup>8</sup>G. Heiland, E. Molwo, and F. Stokmann, in *Solid State Physics*, edited by H. Ehrenreich, F. Seitz, and D. Turnbull (Academic, New York, 1958), Vol. 8, p. 193.

<sup>9</sup>H. J. Krusemeyer, *Phys. Rev.* **114**, 655 (1959), and *J. Phys. Chem. Solids* **23**, 767 (1962).

<sup>10</sup>A. Many, *Crit. Rev. Solid State Sci.* **4**, 515 (1974); D. Eger, Y. Goldstein, and A. Many, *RCA Rev.* **36**, 508 (1975).

<sup>11</sup>Y. Goldstein, A. Many, I. Wagner, and J. Gersten, *Surf. Sci.* **98**, 599 (1980).

<sup>12</sup>J. I. Gersten, *Surf. Sci.* **92**, 579 (1980), and **97**, 206 (1980).

<sup>13</sup>Y. Grinshpan, M. Nitzan, and Y. Goldstein, *Phys. Rev. B* **19**, 1098, 4107 (1979).